Downloaded from geology.gsapubs.org on October 1, 2014

Geology

Slip-tendency analysis and fault reactivation

Alan Morris, David A. Ferrill and D.Brent Henderson

Geology 1996;24;275-278
doi: 10.1130/0091-7613(1996)024<0275:STAAFR>2.3.CO;2

Email alerting services click www.gsapubs.org/cgi/alerts to receive free e-mail alerts when new articles cite this article

Subscribe click www.gsapubs.org/subscriptions/ to subscribe to Geology

Permission request click http://www.geosociety.org/pubs/copyrt.htm#gsa to contact GSA

Copyright not claimed on content prepared wholly by U.S. government employees within scope of their employment. Individual scientists are hereby granted permission, without fees or further requests to GSA, to use a single figure, a single table, and/or a brief paragraph of text in subsequent works and to make unlimited copies of items in GSA's journals for noncommercial use in classrooms to further education and science. This file may not be posted to any Web site, but authors may post the abstracts only of their articles on their own or their organization's Web site providing the posting includes a reference to the article's full citation. GSA provides this and other forums for the presentation of diverse opinions and positions by scientists worldwide, regardless of their race, citizenship, gender, religion, or political viewpoint. Opinions presented in this publication do not reflect official positions of the Society.

Notes

Geological Society of America

THE GEOLOGICAL SOCIETY OF AMERICA

Downloaded from geology.gsapubs.org on October 1, 2014

Slip-tendency analysis and fault reactivation

Alan Morris
Division of Earth and Physical Sciences, University of Texas, San Antonio, Texas 78249-0663
David A. Ferrill
D. Brent Henderson
Center for Nuclear Waste Regulatory Analyses, Southwest Research Institute, 6220 Culebra Road, San Antonio, Texas 78238-5166

ABSTRACT

Slip-tendency analysis is a new technique that permits rapid assessment of stress states and related potential fault activity. The tendency of a surface to undergo slip in a given stress field depends on its frictional characteristics (primarily controlled by rock type) and the ratio of shear to normal stress acting on the surface, here defined as slip tendency (determined by orientation of the surface within the stress field). An interactive computer tool displays the stress tensor in terms of its associated slip-tendency distribution and the relative likelihood and direction of slip on surfaces of all orientations. The technique provides easy visualization and rapid evaluation of stress in terms of its potential for causing slip on individual faults or fault populations for use in seismic-risk and fault-rupture–risk assessment, exploration for high-risk and earthquake-prone blind faults, selection of likely earthquake focal mechanism solutions, and for use in analysis of compatibility of geologic structures.

INTRODUCTION

Earthquakes pose severe risks to population centers or sensitive installations in areas of active faulting. For example, earthquakes near the proposed high-level radioactive waste repository site at Yucca Mountain, Nevada, would pose considerable risk during construction and after closure of the facility. Active faults provide riskier hydrocarbon traps because of the potential for "fault-valve" behavior (Sibson, 1990). Elevated fluid pressure can cause faults to "leak" before stress modification causes the formation of new faults. Here we present a new technique, slip-tendency analysis, to assess slip potential for mapped or suspected faults in a known or inferred stress state.

In most homogeneous stress states, two surfaces are optimally oriented for slip (Anderson, 1951). These surfaces intersect in the direction of the intermediate principal compressive stress (σ_2) and are symmetrical about σ_1 (e.g., Jaeger and Cook, 1979). However, Wallace (1951) showed that the maximum resolved shear stress (magnitude and orientation) on any surface varies continuously with the orientation of the surface in a stress field, and as a function of the relative magnitudes of the principal stresses. Bott (1959) stated explicitly: "the maximum shearing stress within a . . . plane of fracture . . . may lie in every possible direction for a variable stress system of given orientation. . . ." Bott concluded that principal stress rotations out of the vertical and horizontal planes are unnecessary to explain oblique-slip faults.

The distribution of surfaces with high resolved shear stress and the variability of the direction of the maximum resolved shear stress are expressed naturally in several ways. Natural and analogue fault systems tend to be anastomosing networks of slip surfaces with variable orientations. The "Andersonian" conjugate system (Anderson, 1951) tends to dominate, but many surfaces contribute to the overall deformation. Earthquakes and their associated aftershocks also occur on a variety of slip surfaces, and this phenomenon is utilized to determine the tectonic stress state responsible for the earthquake (McKenzie, 1969; Gephart and Forsyth, 1984).

Although well established, the principle of variation in shear stress within the stress tensor is difficult to visualize and is of limited utility as a description of the likelihood that a surface will slip. This likelihood is a function of the frictional resistance on the sliding surface, which is governed by rock properties and the ratio of shear to normal stress on the surface. A more useful perspective for determining the population of surfaces that might reasonably slip in a stress field is to view the ratio of shear to normal stress and the direction of the maximum resolved shear stress. This is the basis of slip-tendency analysis.

SLIP TENDENCY

Slip is likely to occur on a surface when the resolved shear stress, τ, equals or exceeds the frictional resistance to sliding, F, which is proportional to the normal stress, σ_n, acting across that surface (Jaeger and Cook, 1979; Fig. 1). Whether a surface will actually slip depends upon its cohesive strength, if any, and the coefficient of static friction, μ. For a cohesionless fault, at the instant of sliding:

$$F \leq \tau = \mu\sigma_n, \quad (1)$$

and

$$\mu = \tau/\sigma_n. \quad (2)$$

The slip tendency (T_s) of a surface is defined as the ratio of shear stress to normal stress on that surface:

$$T_s = \tau/\sigma_n. \quad (3)$$

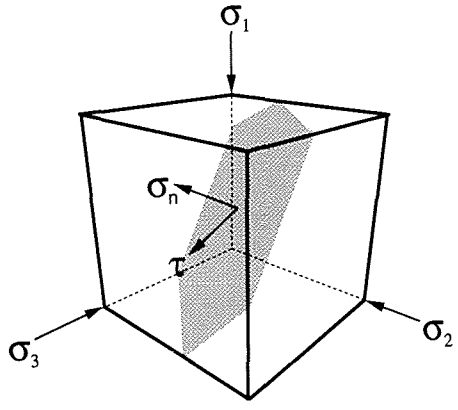

Figure 1. Normal stress, σ_n, and shear stress, τ, on arbitrarily oriented surface within stress field defined by three principal compressive stresses σ_1, σ_2, and σ_3.

Downloaded from geology.gsapubs.org on October 1, 2014

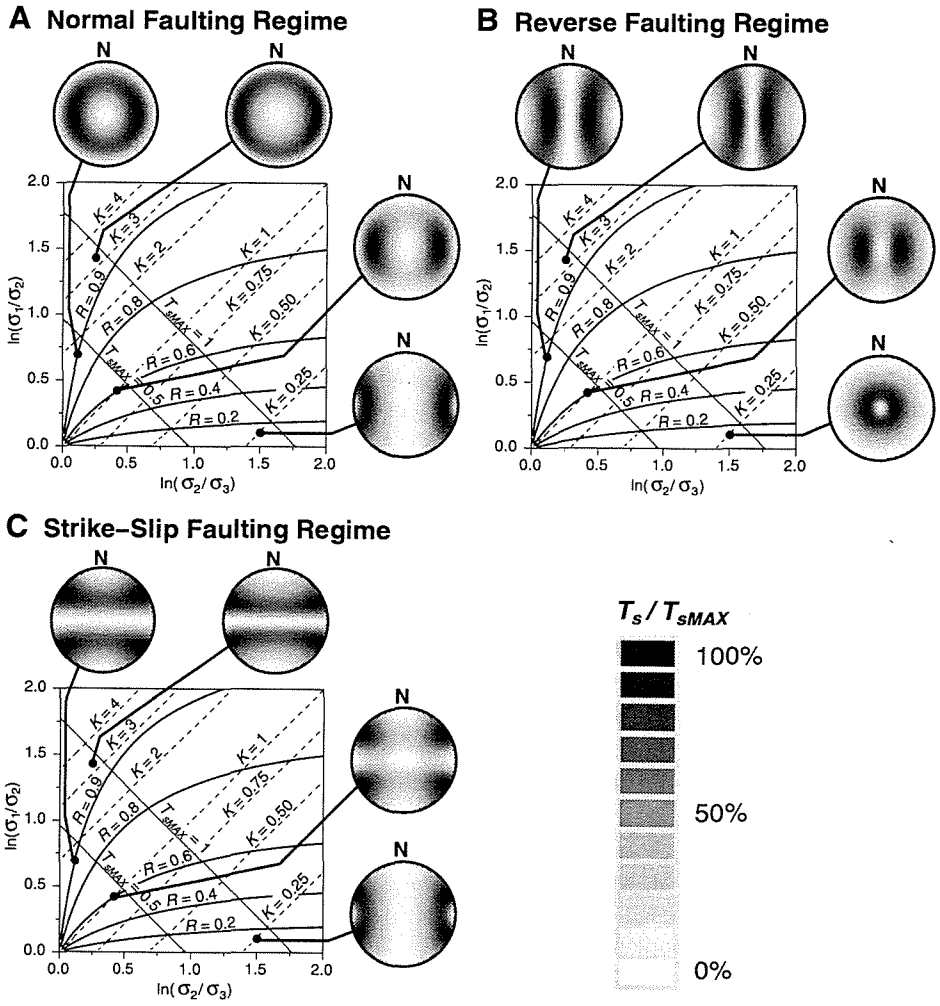

Figure 2. Graphs of $\ln(\sigma_1/\sigma_2)$ vs. $\ln(\sigma_2/\sigma_3)$ with contours of R values (heavy solid lines), K values (dashed lines), and T_{sMAX} (thin solid lines). 0.5 and 1.0 contours of T_{sMAX} bracket most realizable conditions of stress for earth's crust (Byerlee, 1978). A, B, and C: Selected slip tendency plots for four stress states are superimposed on ln/ln graph of σ_1/σ_2 vs. σ_2/σ_3; slip tendency plot is lower hemisphere, equal-angle projection of poles to potential slip surfaces, which are contoured by magnitude of the slip tendencies as percentage of T_{sMAX} (see shade scale). In normal fault regime (A), σ_1 is vertical, σ_2 is north-south, and σ_3 is east-west. In reverse fault regime (B), σ_3 is vertical, σ_2 is north-south, and σ_1 is east-west. In strike-slip fault regime (C), σ_2 is vertical, σ_1 is north-south, and σ_3 is east-west.

The slip tendency depends solely on the stress field (stress tensor) and the orientation of the surface. The coefficient of static friction, μ, is the value of T_s that will cause slip on a cohesionless surface and is often referred to as the fault "strength" in analysis of earthquake focal mechanisms. Should slip occur on a surface with a low T_s, the fault must have a low μ and thus is "weak."

SLIP TENDENCY AND THE STRESS TENSOR

The distribution of slip tendency with fault orientation depends upon the relative values of the principal stresses (Wallace, 1951; Bott, 1959; Fig. 2) and is very sensitive to the axial symmetry of the stress tensor. If the orientations and magnitudes of the principal stresses are known or assumed, it is possible to determine (Bott, 1959; Ramsay, 1967): (1) the normal stress, σ_n; (2) the shear-stress magnitude, τ; and (3) the shear-stress direction, $\vec{\tau}$, in the surface. The magnitudes of the normal and shear stresses determine slip tendency (τ/σ_n), and the direction of the maximum resolved shear stress indicates the likely direction and sense of motion.

The $\vec{\tau}$ field of the stress tensor is most commonly exploited to determine stress states from earthquake data (McKenzie, 1969; Gephart, 1990) and paleoslip data (Angelier, 1979). In these applications, observed or computed slip directions are considered to reflect the orientations of $\vec{\tau}$ within a homogeneous stress tensor. The observed distribution is iteratively compared with the computed $\vec{\tau}$ fields of a wide variety of stress tensors to obtain an optimized best fit. Friction is regarded as secondary in importance or is not considered, although Wesnousky and Jones (1994) examined paired-fault systems for their synergistic qualities by computing states of friction.

We consider the reverse perspective. We have developed an interactive computer tool that specifies the stress tensor by choosing the principal stresses and by calculating and displaying slip-tendency data for surfaces of all orientations. The results can be interactively adjusted by modifying the three principal stresses to investigate slip tendency and direction ($\vec{\tau}$) on any individual surface. This procedure is applied to mapped fault traces to investigate the effects of various stress fields on known or suspected faults.

Slip Tendency, Surface Orientations, and Stress Fields

Stress fields can be described in terms of K and R (the stress difference ratio), where:

$$K = (\sigma_1/\sigma_2)/(\sigma_2/\sigma_3) \quad (5)$$

or

$$K = (\sigma_1\sigma_3)/\sigma_2^2,$$

and

$$R = (\sigma_1 - \sigma_2)/(\sigma_1 - \sigma_3) \quad (6)$$

Stress fields where $K \approx 1$ have strongly bimodal distributions of surfaces with high slip tendencies (Fig. 2, A, B, and C). The distribution of high-slip-tendency surfaces tends toward a girdle about the σ_3 axis, where $K < 1$, and about the σ_1 axis, where $K > 1$ (Fig. 2).

APPLICATIONS

Fault-Pattern Analysis at Yucca Mountain, Nevada

Ideally, the tendency for seismic faulting in a rock volume could be simulated by considering all potential slip surfaces, their surface areas, positions, and geometries. With the exception of some three-dimensional seismic surveys, high-quality data are not commonly available, so the slip tendencies of a population of faults can be approximated by utilizing fault-trace maps and "tuning" the calculations for specific fault dips. Slip-tendency computations are linked to fault-trace maps by changing the proposed stress field. This provides rapid assessment of the compatibility of fault sets for particular stress fields. A consequence of this viewing technique is that faults can be semiquantitatively assessed for their slip potential in a chosen stress field, a first step in

Downloaded from geology.gsapubs.org on October 1, 2014

determining seismic hazard of known or suspected faults.

Stock et al. (1985) provided the only published measurements of the in situ stress state at Yucca Mountain. At depths of between 1 and 1.3 km, their measurements indicate that σ_1 = vertical = 20.8–27.2 MPa (lithostatic based on depth and rock density); σ_2 = N25°E–N30°E = 16.8–17.9 MPa; and σ_3 = N60°W–N65°W = 10.6–14.8 MPa: σ_2 varies from 66% to 81% of σ_1, and σ_3 varies from 47% to 54% of σ_1 (Stock et al., 1985). Extrapolating these percentages to a depth of 5 km and assuming an average rock density of 2.7 g/cm^3, σ_1 = 133 MPa, σ_2 = 88–108 MPa, and σ_3 = 63–72 MPa. Assuming a water-table depth of 600 m (Stock et al., 1985), and interconnecting permeability, hydrostatic pressure at 5 km will be 43 MPa. Thus, effective principal stresses would be: σ_1 = vertical = 90 MPa, σ_2 = N25°E–N30°E = 45–65 MPa (50%–72% of σ_1), and σ_3 = N60°W–N65°W = 20–29 MPa (22%–32% of σ_1), at 5 km beneath Yucca Mountain. Harmsen (1994) obtained an R value of 0.35 for the stress field responsible for the 1992 magnitude 5.6 Little Skull Mountain earthquake (20 km southeast of Yucca Mountain, at a depth of about 10 km). Again, assuming average rock density is 2.7 g/cm^3, water-table depth is 600 m, and reasonable values for μ (0.6–0.9), this is equivalent to σ_1 = 172 MPa, σ_2 = 71%–78% of σ_1, and σ_3 = 14%–38% of σ_1, at 10 km depth. Our estimate for σ_3 below Yucca Mountain (based on measurements by Stock et al., 1985) is within the range derived from Harmsen's (1994) data. Estimates of σ_2 based on the measurements of Stock et al. (1985) and the analysis of Harmsen (1994) only overlap in the range of 71%–72% of σ_1. For the purposes of modeling slip-tendency patterns, we have chosen the high end of our range (σ_2 = 72% of σ_1) in order to be consistent with both data sets. Applying the stress field, σ_1 = vertical = 90 MPa, σ_2 = N25°E–N30°E = 65 MPa, and

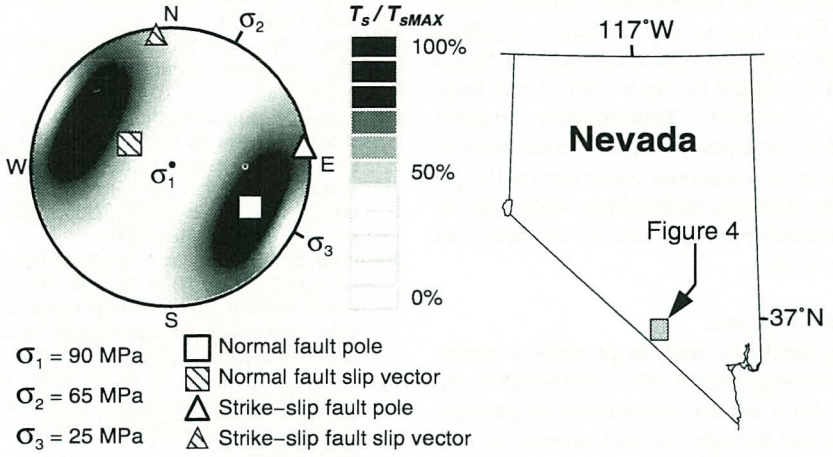

Figure 3. Slip-tendency plot showing that both dip-slip and strike-slip faults with certain orientation ranges have high slip tendencies in contemporary stress field at Yucca Mountain, Nevada.

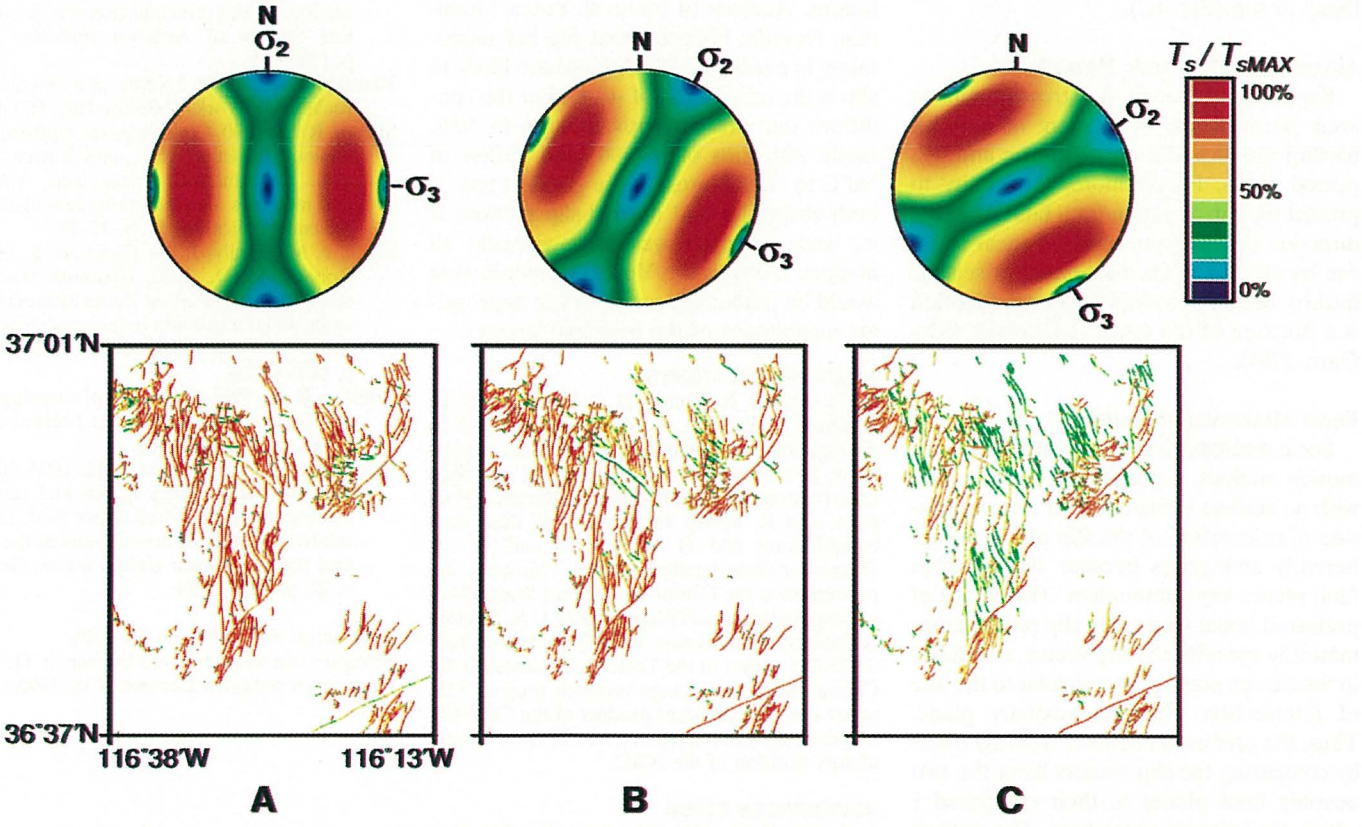

Figure 4. Slip-tendency plots and associated fault trace maps for three orientations of contemporary principal stresses at Yucca Mountain, Nevada. Fault traces (after Frizzel and Shulters, 1990) are color coded according to same scale as slip-tendency plots. Faults are all assumed to dip 65°–80°. A: σ_1, vertical, σ_2, north-south, σ_3, east-west; B: σ_1, vertical, σ_2, N28°E, σ_3, N62°W; C: σ_1, vertical, σ_2, N60°E, σ_3, N30°W.

Downloaded from geology.gsapubs.org on October 1, 2014

σ_3 = N60°W–N65°W = 25 MPa, to the faults of Yucca Mountain shows that both strike-slip and normal faults can coexist (Fig. 3). Moderately to steeply dipping faults with north-south to northeast-southwest strikes tend to have high slip tendencies (Fig. 4B). These conclusions agree with those of Stock et al. (1985). Many faults are in orientations of relatively high slip tendency; however, several large northwest-southeast–trending faults have orientations of low slip tendency and are not in favorable orientations for contemporary slip. Consequently, we infer that these faults developed under different stress conditions and that the stress field at Yucca Mountain has evolved from a previous state, similar to that illustrated in Figure 4A.

All likely Yucca Mountain stress states have K values of ~0.6–0.8 and R values of ~0.4–0.62. Under these conditions, surfaces with high slip tendency have tight bimodal or small-circle girdle distributions about σ_3 (Fig. 2A). As a result, the orientation of σ_3 strongly controls orientation of likely active faults. For example, if σ_3 is horizontal, trending N90°W, almost all faults with dips of 65°–80° at Yucca Mountain have high slip tendency (Fig. 4A). However, if σ_3 is rotated to N30°W, many faults with high slip tendencies would become less likely to slip (Fig. 4C).

Assessment of Seismic Hazard

Knowledge of the in situ stress state in an area permits the evaluation of relative earthquake hazard for both known and suspected faults. Furthermore, the ability to predict the slip direction for a fault from the direction of maximum resolved shear stress can be used to refine assessment of seismic hazard, because earthquake ground motion is a function of the sense of fault slip (McGarr, 1984).

Focal Mechanism Solutions

Focal mechanism solutions based on first-motion analysis, especially for earthquakes with no surface break or other clear indication of orientation of the slip plane, are inherently ambiguous because two possible fault planes explain the data. The choice of preferred nodal plane (the slip plane) automatically specifies the slip vector, which lies in the chosen plane perpendicular to the line of intersection with the auxiliary plane. Thus, the preferred choice is typically made by comparing the slip vectors from the two possible fault planes to their computed $\vec{\tau}$ within the inferred stress field. The surface with the smaller angular difference between its slip and shear stress vectors is chosen as the preferred nodal plane. One commonly used stress-inversion method for use with earthquake data, the focal mechanism stress inversion (FMSI) model (Gephart, 1990), specifically optimizes the focal-mechanism slip-vector data with the shear-stress vector component ($\vec{\tau}$) of the assumed stress tensor. Therefore, the FMSI model relies solely on the slip-direction criterion to obtain a best-fit stress tensor. Such calculations can produce anomalous results in the form of assumed slip on misoriented surfaces (those with low values of slip tendency). Gephart (1990) suggested that a frictional criterion could be added to the model to eliminate such anomalies. Slip-tendency analysis could be incorporated into a model such as FMSI as an additional constraint on the selection of slipped nodal planes and as part of the optimization process to estimate the stress tensor.

CONCLUSIONS

Slip-tendency analysis provides a means for assessing relative risk of earthquakes and fault slip, a test for compatibility of geologic structures thought to have developed in a single stress field, a new approach to exploration for high-risk and earthquake-prone blind faults, and an alternative (to shear-stress vector orientations) for interpretation of slipped faults from focal-mechanism solutions. Analysis of faults at Yucca Mountain, Nevada, indicates that the key uncertainty in predicting which faults are likely to slip is the orientation of σ_3. Under the conditions that are currently thought to exist, faults with dips of 60°–90° and strikes of N0°E to N30°E present the greatest risk of both strike-slip and normal-slip motion. If σ_3 were oriented west-east, virtually all mapped faults in the Yucca Mountain area would be potentially active, given appropriate magnitudes of the principal stresses.

ACKNOWLEDGMENTS

We thank S. R. Young, H. L. McKague, R. B. Hoffman, B. Sagar, J. A. Stamatakos, and M. L. Zoback for encouragement and critical suggestions; S. Walnum and C. Fleming for contributions to programming; R. Klar, R. Martin, J. Foegelle, and K. Spivey for the use of their data compilations; and H. T. Mullins and W. M. Dunne for their detailed reviews. This work was performed at the Center for Nuclear Waste Regulatory Analyses (CNWRA) under U.S. Nuclear Regulatory Commission (NRC) contract NRC-02-93-005 as part of the Tectonic Processes in the Central Basin and Range research project. This paper is an independent product of the CNWRA and does not necessarily reflect the views or regulatory position of the NRC.

REFERENCES CITED

Anderson, E. M., 1951, The dynamics of faulting and dyke formation with applications to Britain: Edinburgh, United Kingdom, Oliver and Boyd, 206 p.

Angelier, J., 1979, Determination of the mean principal directions of stresses for a given fault population: Tectonophysics, v. 56, p. T17–T26.

Bott, M. H. P., 1959, The mechanics of oblique slip faulting: Geological Magazine, v. 96, p. 109–117.

Byerlee, J. D., 1978, Friction of rocks: Pure and Applied Geophysics, v. 116, p. 615–626.

Frizzel, V. A., Jr., and Shulters, J., 1990, Geologic map of the Nevada Test Site, southern Nevada: U.S. Geological Survey Miscellaneous Investigations Series Map I-2046, scale 1:100,000.

Gephart, J. W., 1990, Stress and the direction of slip on fault planes: Tectonics, v. 9, p. 845–858.

Gephart, J. W., and Forsyth, D. W., 1984, An improved method for determining the regional stress tensor using earthquake mechanism data: Application to the San Fernando earthquake sequence: Journal of Geophysical Research, v. 89, p. 9305–9320.

Harmsen, S. C., 1994, The Little Skull Mountain, Nevada, earthquake of 29 June 1992: Aftershock focal mechanisms and tectonic stress field implications: Seismological Society of America Bulletin, v. 84, p. 1484–1505.

Jaeger, J. C., and Cook, N. G. W., 1979, Fundamentals of rock mechanics (third edition): London, United Kingdom, Chapman and Hall, 593 p.

McGarr, A., 1984, Scaling of ground motion parameters, state of stress, and focal depth: Journal of Geophysical Research, v. 89, p. 6969–6979.

McKenzie, D. P., 1969, The relation between fault plane solutions for earthquakes and the directions of the principal stresses: Seismological Society of America Bulletin, v. 59, p. 591–601.

Ramsay, J. G., 1967, Folding and fracturing of rocks: New York, McGraw Hill, 560 p.

Sibson, R. H., 1990, Conditions for fault-valve behaviour, *in* Knipe, R. J., and Rutter, E. H., eds., Deformation mechanisms, rheology and tectonics: Geological Society of London Special Publication 54, p. 15–28.

Stock, J. M., Healy, J. H., Hickman, S. H., and Zoback, M. D., 1985, Hydraulic fracturing stress measurements at Yucca Mountain, Nevada, and relationship to regional stress field: Journal of Geophysical Research, v. 90, p. 8691–8706.

Wallace, R. E., 1951, Geometry of shearing stress and relationship to faulting: Journal of Geology, v. 59, p. 111–130.

Wesnousky, S. G., and Jones, C. H., 1994, Oblique slip, slip partitioning, spatial and temporal changes in the regional stress field, and the relative strength of active faults in the Basin and Range, western United States: Geology, v. 22, p. 1031–1034.

Manuscript received June 12, 1995
Revised manuscript received December 11, 1995
Manuscript accepted December 19, 1995